ISSN (Online): 2455-7838
SJIF Impact Factor (2017): 5.705

EPRA International Journal of

Research & Development

(IJRD)

Monthly Peer Reviewed & Indexed International Online Journal

Volume: 3, Issue:10, October 2018

Published By :
EPRA Journals

SJIF Impact Factor: 5.705 Volume: 3 | Issue: 10 |October| 2018 ISSN: 2455-7838(Online)
EPRA International Journal of Research and Development (IJRD)

EFFECT OF SLIP BOUNDARY CONDITIONS ON MHD NANOFLUID FLOW

P K Pattnaik[1]
[1]Department of Mathematics, College of Engg. and Technology, Bhubaeswar, 751029, Odisha, India

N Mishra[2]
[2]Department of Mathematics, College of Engg. and Technology, Bhubaeswar, 751029, Odisha, India

M M Muduly[3]
[3]Department of Mathematics, College of Engg. and Technology, Bhubaeswar, 751029, Odisha, India

ABSTRACT

In this examination, the boundary layer flow ad heat transfer over a porous stretching sheet due to a nanofluid with the impacts of magnetic field, slip boundary condition and thermal radiation have been explored. The trasport conditions utilized in the examination considered the impact of Brownian motion ad thermophoresis parameters. The solution for the velocity, temperature ad nanoparticle concentration depends upon parameters viz. thermal radiation parameter (R), *Prandtl number* (P_r), *Lewis number* (L_e), *Brownian motion parameter* (N_b), *thermophoresis parameter* (N_t), *Eckert number* (E_c), *magnetic parameter* (M) *ad slip parameters. Similarity transformation is utilized to change over the governing non-linear boundary layer conditions into coupled higher order ordinary differential equations. These equations are numerically tackled utilizing fourth order Runge–Kutta method alongwith shooting technique. An examination has been done to explain the impacts of governing parameters relating to different physical conditions. Numerical results are gotten for appropriations of velocity, temperature ad concentration, and in addition, for the skin friction, local Nusselt number and local Sherwood number for a few benefits of governing parameters. The results demonstrate that the local Nusselt number declines with an increasing values in both Brownian motion parameter* (N_b) *ad thermophoresis parameter* (N_t). *However, the local Sherwood number increases with an increase in both thermophoresis parameter* (N_t) *ad Lewis number* (L_e), *but it decreases as the values of* (N_b) *increase. Besides, it was found that the surface temperature of the sheet increases with an increase in the Eckert number* (E_c). *An examination with past investigations accessible in the writing has been done ad we found an amazing concurrence with it.*

KEYWORDS: *Nanofluid; Stretching sheet; Slip boundary conditions; Brownian motion; Thermophoresis; Heat transfer.*

Nomenclature

a	positive constant	R	thermal radiation parameter
A	velocity slip parameter	Re_x	local Reynolds number
B	thermal slip parameter	S	suction parameter
B_0	magnetic field	Sh_x	local Sherwood number
c	solutal slip parameter	T	temperature of the fluid
C	concentration of the fluid	T_w	surface temperature
C_{fx}	local skin friction	T_∞	ambient temperature
c_p	specific heat at constant pressure	u, v	velocity components in
C_w	surface concentration		x, y direction
C_∞	ambient concentration	u_w	stretching velocity
D_B	Brownian diffusion coefficient	x, y	horizontal and vertical coordinate
D_T	thermophoretic diffusion coefficient	**Greek symbols**	
E_c	Eckert number	α	thermal diffusivity
f	dimensionless flow function	τ	relative heat capacity
K_1	temperature slip factor	υ	kinematic viscosity
K_2	concentration slip factor	μ	dynamic viscosity
k	thermal conductivity	ρ_f	density of the base fluid
k^*	Rosseland mean spectral absorption	ρ_p	density of the nanoparticles
	coefficient	$(\rho c_p)_p$	heat capacity of the nanoparticle
L	velocity slip factor	$(\rho c_p)_f$	heat capacity of the base fluid
L_e	Lewis number	σ	electrical conductivity
M	magnetic parameter	σ^*	Stefan-Boltzmann constant
N_b	Brownian motion parameter	θ	dimensionless temperature
N_t	thermophoresis parameter	ϕ	dimensionless concentration
Nu_x	local Nusselt number	τ_w	skin friction coefficient
$\mathrm{P_r}$	Prandtl number		
q_r	thermal radiative heat flux	**Subscripts**	
q_m	mass flux at the surface	∞	condition at the free flow
q_w	heat flux at the surface	w	condition at the surface

1. INTRODUCTION

The boundary layer flow over a stretching sheet in a uniform flow of fluid has been considered broadly in fluid mechanics. Countless has been done on the zone of the boundary layer flow over a moving consistent stretching sheet in the perspective of its various modern ad designing applications. A portion of the wide application zones we have run over are in the flowline expulsion of plastic sheet, in metallurgy, cooling of a boundary less metallic plate in a cooling shower, polymer expulsion, cooling or drying of papers ad in material ad glass fibre generation. Flow ad heat transfer qualities over a stretching sheet have vital modern applications, for example, in the expulsion of a polymer sheet from a pass on. In the assembling of such sheets, the liquefy issues from an opening ad is thusly extended. The rates of stretching ad cooling affect the nature of the last item with wanted attributes. The previously mentioned procedures include cooling of a fluid by illustration into a cooling framework. The properties wanted for the result of such process predominately rely upon two attributes: the first is the cooling fluid utilized and the other is the rate of stretching. Fluids of non-Newtonian qualities with feeble electrical conductivity ca be decided for as a cooling fluid as their flow and subsequently the heat transfer rate ca be directed through some outer means. Ideal rate of stretching is essential, as quick stretching results in sudden cementing, along these lines crushing the properties anticipated from the item. After the spearheading work of Sakiadis [1], an extensive number of research papers on a stretching sheet have been distributed by considering different governing parameters, for example, suction/infusion, porosity, magnetic field parameter and radiation with various sorts of fluids, for example, Newtonian and some non-Newtonian polar, ad couple pressure fluids. Be that as it may, the plentiful writing on the boundary layer flow over a stretching sheet is restricted to Newtonian ad some non-Newtonian fluids flow with customary no-slip flow boundary condition over different stretching geometry, for example, direct ad non-linear stretching sheet ad a little consideration was given to stretching sheet with slip boundary condition. Nonetheless, fluids with smaller scale or nano-scale measurements have flow conduct that extraordinarily contrasts from the customary fluid flow qualities ad has a place with the slip flow administration. For the flow in the slip administration, the smooth motion still complies with the Navier– Stoke's conditions, however with slip velocity, temperature ad concentration boundary conditions. For example, the flow in numerous utilizations of small scale/nano frameworks, for example, hard plate drive, miniaturized scale pump, smaller scale valve ad miniaturized scale spouts is in slip progress administration, or, in other words slip boundary at the divider. The no-slip boundary condition is known as the fundamental appearance of the Navier– Stoke's hypothesis of fluid elements. Yet, there are circumstances wherein such condition isn't suitable. Particularly no-slip condition is lacking for most non-Newtonian fluids ad nanofluids, as some polymer liquefy regularly demonstrates tiny divider slip ad that when all is said in done is administered by a non-direct ad monotone connection between the slip velocity ad the footing. The fluids showing boundary slip discover applications in mechanical issues, for example, clearing of counterfeit heart valves and interior cavities. The prior examinations that considered the slip boundary condition over a stretching sheet were led by Adersson [2]. He gave a shut shape arrangement of a full Navier– Stokes conditions for a magneto hydrodynamics flow over a stretching sheet. Following Adersson, Wag [3] found the shut frame similitude arrangement of a full Navier– Stoke's conditions for the flow because of a stretching sheet with fractional slip. Besides, Wag [4] researched stagnation slip flow ad heat transfer on a moving plate. Also, Fag et al. [5] examined slip magneto hydrodynamics gooey flow over a stretching sheet logically. Even more, Hayat et al. [6] extended the issue of the past analysts by joining thermal slip condition ad examined insecure magneto hydrodynamic flow ad heat transfer over a penetrable stretching sheet with slip condition. Also, Aziz [7] examined hydrodynamic ad thermal slip boundary layer flow over a level plate with steady heat transition boundary condition. The previously mentioned writing examined the slip boundary conditions when the primary order velocity slip boundary conditions were utilized. Be that as it may, Fag et al. [8] found a shut shape answer for gooey flow over a contracting sheet utilizing the second order velocity slip flow display. Also, Mahantesh et al. [9] examined flow ad heat transfer over a stretching sheet by considering second order velocity slip boundary condition. Nanofluids are the suspension of nanometre measured strong particles ad strands, which have been proposed as a methods for upgrading the execution of heat transfer fluids presently accessible, for example, water, toluene, oil and ethylene glycol blend. Nanofluids have gotten the enthusiasm of numerous specialists as of late as a result of their incredibly upgraded thermal conductivity property [10]. One ca allude crafted by creators [11– 13] with respect to the thermal conductivity improvement of the nanofluids accessible in the writing. These days, the investigation of convective heat move in nanofluids wind up dynamic research territory because of its heat transfer improvement attributes. As a result of the way that cooling is one of the specialized difficulties confronted numerous ventures including microelectronic, transportation, strong state lighting ad assembling; the possibility of nanofluid has been proposed as a methods for mitigating these difficulties. The boundary layer flow ad heat transfer due to nanofluids over a stretching sheet are a pushed regions of flow look into. Such examinations

discover applications over an expansive rage of science and designing controls. An imperative part of boundary layer flow of a nanofluid over a stretching sheet is the heat transfer qualities. It is critical to comprehend the heat transfer attributes of the stretching sheet with the goal that the completed item meets the coveted quality. This is because of the way that the nature of a last item depends upon the rate of heat transfer at the stretching surface. In like manner, Kuznetsov and Nield [14] have contemplated the normal convective boundary layer flow of a nanofluid past a vertical plate diagnostically. They utilized a model in which Brownian motion and thermophoresis impacts were considered. Additionally, Kha ad Pop [15] utilized a similar model to think about the boundary layer flow of a nanofluid past a stretching sheet with a steady surface temperature. Recently Ibrahim ad Shaker [16] have examined the boundary layer flow ad heat transfer of nanofluid over a vertical Plate considering the convective surface boundary condition. As of late, Haddad et al. [17] tentatively examined normal convection in nanofluid by considering the job of thermophoresis ad Brownian motion in heat transfer upgrade. They showed that ignoring the job of Brownian motion ad thermophoresis fall apart the heat transfer ad this crumbling hoists when the volume part of a nanoparticles increments. Additionally, Bachok et al. [18] numerically considered unfaltering boundary layer flow of a nanofluid over a moving semi-endless plate in a uniform free flow. Further, Makinde ad Aziz [19] directed a numerical investigation of boundary layer flow of a nanofluid past a stretching sheet with convective boundary condition. Likewise, Vajravelu et al. [20] examined the convective heat move in a nanofluid flow over a stretching surface utilizing Ag– water or Cu– water nanofluid. Besides, Hamad ad Ferdows [21] contemplated boundary layer stagnation point flow towards a thermal permeable stretching sheet soaked with a nanofluid with heat assimilation/age ad suction/blowing utilizing Lie assemble examination. Thus, Mustafa et al. [22] examined stagnation point flow of a nanofluid towards a stretching sheet. Wubshet et al. [23] were additionally numerically researched the MHD stagnation point flow of a nanofluid towards a stretching sheet. Also, magnetic consequences with the expectation of complimentary convection flow of a nanofluid past a vertical semi-unbounded level plate have been examined by Hamad et al. [24]. All things considered, Yacob et al. [25] have additionally investigated the boundary layer flow ad heat transfer applying a convective boundary condition to the issue of flow over level plate. MHD slip flow, heat and mass move in nanofluids over a porous stretching/contracting surface logically examined by [26]. In addition, Uddin et al. [27] broke down scaling bunch change for MHD boundary layer slip flow of a nanofluid over a convectively thermal stretching sheet with heat age.

The thorough survey of nanofluids about hypothetical ad numerical examination, trials ad applications were depicted by Wag ad Mujumdar [28, 29]. They talked about the hypothetical examination, readiness ad utilizations of the nanofluids. The aforementioned considers examined the boundary layer flow of nanofluids by ignoring the slip boundary condition in the flow investigation. Recently, Aminreza et al. [30] ad Kalidas [31] numerically examined the impact of halfway slip boundary condition on the flow ad heat transfer of a nanofluid past a stretching sheet. They demonstrated that the diminished Nusselt number ad Sherwood number are emphatically affected by the slip parameter. Pattnaik et al. [32-36] concentrated the conduct of MHD fluid flow and watched some fascinating results. All the above investigations thought about the no-slip thermal and solutal boundary condition. Be that as it may, there may be a characteristic circumstance where no-slip boundary condition may not be relevant. In such circumstances, we may be forced to consider slip boundary condition. Therefore, this study try to fulfil this gap.

In this paper we considered the slip boundary conditions in velocity, temperature ad concentration to examine the boundary layer flow ad heat transfer investigation of a nanofluid. Henceforth, the reason for this examination is to round this learned about information hole in the nanofluid. The examination investigations magneto hydrodynamics boundary layer flow over a stretching sheet in nanofluid with the incorporation of radiation impact. Besides, the joined impacts of Brownian motion, thermophoresis parameter ad nanoparticle division on boundary layer flow ad heat transfer because of nanofluid are analysed.

2. MATHEMATICAL FORMULATION

Consider a two-dimensional steady state boundary layer flow of a nanofluid over stretching sheet with surface temperature (T_w) ad concentration (C_w). The stretching velocity of the sheet is $u_w = ax$. Let the wall mass transfer be (V_w), which will be determined later. The flow is assumed to be generated by stretching sheet issuing from a thin slit at the origin. The sheet is then stretched in such a way that the velocity at any point on the sheet becomes proportional to the distance from the origin. The ambient temperature ad concentration, respectively, are (T_∞) ad (C_∞). The flow is subjected to the combined effect of thermal radiation ad a transverse

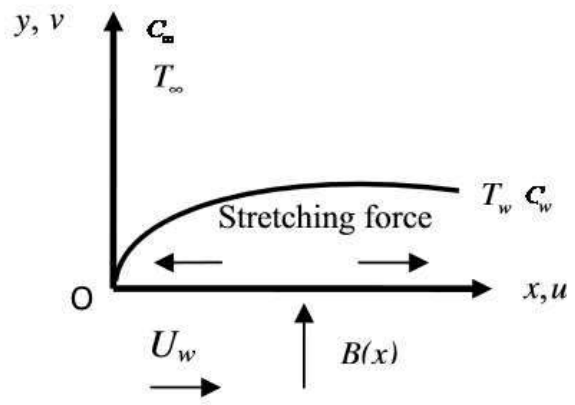

Fig. 1 Flow diagram

magnetic field of strength (B_0), which is assumed to be applied in the positive $y-$direction, normal to the surface. The induced magnetic field is also assumed to be small compared to the applied magnetic field; so it is neglected. It is further assumed that the base fluid and the suspended nanoparticles are in thermal equilibrium. It is chosen that the coordinate system $x-$axis is along stretching sheet ad $y-$axis is normal to the sheet.

Under the above assumptions, the governing equation ca be expressed as:

$$\frac{\partial u}{\partial x}+\frac{\partial v}{\partial y}=0 \tag{1}$$

$$u\frac{\partial u}{\partial x}+v\frac{\partial u}{\partial y}=\frac{-1}{\rho_f}\frac{\partial p}{\partial x}+\upsilon\left(\frac{\partial^2 u}{\partial x^2}+\frac{\partial^2 u}{\partial y^2}\right)-\frac{\sigma B_0^2}{\rho_f}u \tag{2}$$

$$u\frac{\partial v}{\partial x}+v\frac{\partial v}{\partial y}=\frac{-1}{\rho_f}\frac{\partial p}{\partial y}+\upsilon\left(\frac{\partial^2 v}{\partial x^2}+\frac{\partial^2 v}{\partial y^2}\right)-\frac{\sigma B_0^2}{\rho_f}v \tag{3}$$

$$\begin{aligned}u\frac{\partial T}{\partial x}+v\frac{\partial T}{\partial y}=&\alpha\left(\frac{\partial^2 T}{\partial x^2}+\frac{\partial^2 T}{\partial y^2}\right)-\frac{1}{(\rho c)_f}\frac{\partial q_r}{\partial y}+\frac{\mu}{\rho c_p}\left(\frac{\partial u}{\partial y}\right)^2+\left(\frac{\sigma B_0^2}{\rho c_p}\right)u^2\\&+\tau\left\{D_B\left(\frac{\partial C}{\partial x}\frac{\partial T}{\partial x}+\frac{\partial C}{\partial y}\frac{\partial T}{\partial y}\right)+\frac{D_T}{T_\infty}\left[\left(\frac{\partial T}{\partial x}\right)^2+\left(\frac{\partial T}{\partial y}\right)^2\right]\right\}\end{aligned} \tag{4}$$

$$u\frac{\partial C}{\partial x}+v\frac{\partial C}{\partial y}=D_B\left(\frac{\partial^2 C}{\partial x^2}+\frac{\partial^2 C}{\partial y^2}\right)+\frac{D_T}{T_\infty}\left(\frac{\partial^2 T}{\partial x^2}+\frac{\partial^2 T}{\partial y^2}\right) \tag{5}$$

The boundary conditions are:

$$\begin{aligned}&u=u_w+L\frac{\partial u}{\partial y}, v=V_w, T=T_w+K_1\frac{\partial T}{\partial y}, C=C_w+K_2\frac{\partial C}{\partial y} \text{ at } y=0\\&u\to U_\infty=0, \quad T\to T_\infty, \quad C\to C_\infty \qquad \text{as } y\to\infty\end{aligned} \tag{6}$$

where $T_w=T_\infty+B\left(\frac{x}{l}\right)^2, C_w=C_\infty+c\left(\frac{x}{l}\right)^2$.

When $L=K_1=K_2=0$, the no-slip condition is recovered. The above boundary condition is valid when $x\square\ l$ which occurs very near to the slit.

Using an order magnitude analysis of the $y-$direction momentum equation (normal to the sheet) and the usual boundary layer approximations, such as:

$$u \gg v,\ \frac{\partial u}{\partial y} \gg \frac{\partial u}{\partial x}, \frac{\partial v}{\partial x}, \frac{\partial v}{\partial y} \text{ and } \frac{\partial p}{\partial y} = 0 \tag{7}$$

After boundary-layer approximation, the governing equations are reduced to:

$$\frac{\partial u}{\partial x} + \frac{\partial v}{\partial y} = 0 \tag{8}$$

$$u\frac{\partial u}{\partial x} + v\frac{\partial u}{\partial y} = \upsilon\frac{\partial^2 u}{\partial y^2} - \frac{\sigma B_0^2}{\rho_f}u \tag{9}$$

$$\begin{aligned} u\frac{\partial T}{\partial x} + v\frac{\partial T}{\partial y} &= \alpha\frac{\partial^2 T}{\partial y^2} - \frac{1}{(\rho c)_f}\frac{\partial q_r}{\partial y} + \frac{\mu}{\rho c_p}\left(\frac{\partial u}{\partial y}\right)^2 \\ &+ \left(\frac{\sigma B_0^2}{\rho c_p}\right)u^2 + \tau\left\{D_B\frac{\partial C}{\partial y}\frac{\partial T}{\partial y} + \frac{D_T}{T_\infty}\left(\frac{\partial T}{\partial y}\right)^2\right\} \end{aligned} \tag{10}$$

$$u\frac{\partial C}{\partial x} + v\frac{\partial C}{\partial y} = D_B\frac{\partial^2 C}{\partial y^2} + \frac{D_T}{T_\infty}\frac{\partial^2 T}{\partial y^2} \tag{11}$$

$$\text{where } \alpha = \frac{k}{(\rho c)_f}, \tau = \frac{(\rho c)_p}{(\rho c)_f}, \upsilon = \frac{\mu}{\rho_f}. \tag{12}$$

Introducing the following dimensionless quantities, the mathematical analysis of the problem is simplified by using similarity transforms:

$$\psi = \sqrt{a\upsilon}\, x f(\eta), \eta = \sqrt{\frac{a}{\upsilon}}\, y, \theta(\eta) = \frac{T - T_\infty}{T_w - T_\infty}, \phi(\eta) = \frac{C - C_\infty}{C_w - C_\infty} \tag{13}$$

The equation of continuity is satisfied if a flow function $\psi(x, y)$ is chosen as:

$$u = \frac{\partial \psi}{\partial y} \text{ and } v = -\frac{\partial \psi}{\partial x} \tag{14}$$

The radiative heat flux in the x-direction is considered negligible as compared to y-direction. Hence, by using Rosseland approximation for radiation, the radiative heat flux is given by,

$$q_r = -\frac{4\sigma^*}{3k^*}\frac{\partial T^4}{\partial y} \tag{15}$$

We assume that the temperature difference with in the flow is sufficiently small such that the term T^4 may be expressed as a linear function of temperature. This is done by expanding T^4 in a Taylor series about a free flow temperature T_∞ as follows:

$$T^4 = T_\infty^4 + 4T_\infty^3(T - T_\infty) + 6T_\infty^2(T - T_\infty)^2 + \ldots \tag{16}$$

Neglecting higher-order terms in the above Eq. (16) beyond the first order in $(T - T_\infty)$, we get:

$$T^4 \cong 4T_\infty^3 T - 3T_\infty^4 \tag{17}$$

Thus, substituting Eq. (17) into Eq. (15), we get:

$$\frac{\partial q_r}{\partial y} = -\frac{16T_\infty^3 \sigma^*}{3k^*}\frac{\partial^2 T}{\partial y^2} \tag{18}$$

Using the similarity transformation quantities, the governing Eqs. (8)–(11) are transformed to the ordinary differential equation as follows:

$$f''' + ff'' - (f')^2 - Mf' = 0 \tag{19}$$

$$\frac{1}{P_r}\left(1+\frac{4}{3}R\right)\theta'' + (f\theta' - 2f'\theta) + E_c(f'')^2 + ME_c(f')^2 + N_b\theta'\phi' + N_t(\theta')^2 = 0 \tag{20}$$

$$\phi'' + L_e(f\phi' - f'\phi) + \frac{N_t}{N_b}\theta'' = 0 \tag{21}$$

The boundary conditions (6) take the form,

$$\left.\begin{aligned} &f(0) = S,\ f'(0) = 1 + Af''(0), \theta(0) = 1 + B\theta'(0), \phi(0) = 1 + c\phi'(0) \\ &f'(\infty) \to 0,\quad \theta(\infty) \to 0,\quad \phi(\infty) \to 0 \end{aligned}\right\} \tag{22}$$

where $M = \dfrac{\sigma B_0^2}{a\rho_f}, \mathrm{P_r} = \dfrac{\upsilon}{\alpha}, N_t = \dfrac{(\rho c)_p D_T (T_w - T_\infty)}{(\rho c)_f \upsilon T_\infty}, N_b = \dfrac{(\rho c)_p D_B (C_w - C_\infty)}{(\rho c)_f \upsilon}$

$$R = \frac{4\sigma^* T_\infty^3}{kk^*}, L_e = \frac{\alpha}{D_B}, E_c = \frac{u_w^2}{c_p(T_w - T_\infty)}, A = L\sqrt{\frac{a}{\upsilon}}, B = K_1\sqrt{\frac{a}{\upsilon}}, c = K_2\sqrt{\frac{a}{\upsilon}} \tag{23}$$

The important physical quantities of interest in this problem are denoted as:

$$C_{fx} = \frac{\tau_w}{\rho u_w^2}, Nu_x = \frac{xq_w}{k(T_w - T_\infty)}, Sh_x = \frac{xq_m}{D_B(C_w - C_\infty)} \tag{24}$$

where $\tau_w = \mu\left(\dfrac{\partial u}{\partial y}\right)_{y=0}, q_w = -k\left(\dfrac{\partial T}{\partial y}\right)_{y=0}, q_m = -D_B\left(\dfrac{\partial C}{\partial y}\right)_{y=0}$ (25)

By using the above equations, we get:

$$C_{fx}\sqrt{\mathrm{Re}_x} = f''(0), \frac{Nu_x}{\sqrt{\mathrm{Re}_x}} = -(1+R)\theta'(0), \frac{Sh_x}{\sqrt{\mathrm{Re}_x}} = -\phi'(0) \tag{26}$$

where $\sqrt{\mathrm{Re}_x} = \dfrac{u_w x}{\upsilon}$.

3. NUMERICAL SOLUTION

An efficient fourth order Runge–Kutta method along with shooting technique has been employed to study the flow model for the above coupled non-linear ordinary differential equations Eqs. (19)–(21) for different values of various governing parameters. The non-linear differential equations are first decomposed into a system of first order differential equation. The coupled ordinary differential Eqs. (19)–(21) are third order in f ad second order in θ ad ϕ which have been reduced to a system of seven simultaneous equations for seven unknowns. In order to numerically solve this system of equations using Runge–Kutta method, the solution requires seven initial conditions but two initial conditions in f one initial condition in each of θ ad ϕ are known. However, the values of f', θ and ϕ are known at $\eta \to \infty$. These end conditions are utilized to produce unknown initial conditions at $\eta \to 0$ by using shooting technique. The most important step of this scheme is to choose the appropriate finite value

of η_∞. Thus to estimate the value of η_∞, we start with some initial guess value ad solve the boundary value problem consisting of Eqs. (19)– (21) to obtain $f''(0), \theta'(0)$ and $\phi'(0)$. The solution process is repeated with another larger value of η_∞ until two successive values of $f''(0), \theta'(0)$ and $\phi'(0)$ differ only after desired significant digit. The last value η_∞ is taken as the finite value of the boundary η_∞ for the particular set of physical parameters for determining velocity, temperature ad concentration, respectively, are $f(\eta), \theta(\eta)$ and $\phi(\eta)$ in the boundary layer. After getting all the initial conditions we solve this system of simultaneous equations using fourth order Runge–Kutta integration scheme. The value of η_∞ is selected to vary from 5 to 12 depending on the physical parameters governing the flow so that no numerical oscillation would occur. Thus, the coupled boundary value problem of third-order in f, second-order in θ ad ϕ has been reduced to a system of seven simultaneous equations of first-order for seven unknowns. In this study, the boundary value problem is first converted into an initial value problem (IVP). Then the IVP is solved by appropriately guessing the missing initial value using the shooting method for several sets of parameters. The step size h = 0.1 is used for the computational purpose. The error tolerance of 10^{-7} is also being used. The results obtained are presented through graphs and the main features of the problems are discussed ad analysed.

4. RESULTS AD DISCUSSION

The numerical solutions are obtained for velocity, temperature ad concentration profiles for different values of governing parameters. The obtained results are displayed through graphs. Fig. 2(a-c) displays the variation in velocity profile for different values of magnetic field parameter (M), mass suction parameter (S) ad velocity slip parameter (A). Fig. 2(a) reveals the influences of magnetic field on the flow field. The presence of transverse magnetic field sets in Lorentz force effect, which results in the retarding effect on the velocity field. As the values of M increase, the retarding force increases and consequently the velocity decreases. The graph also reveals that the boundary layer thickness reduces as magnetic parameter M increases. Figs. 2(b) ad (c) display the distinction of velocity profile with respect to the variation in S ad A. On observing these figures, as the values of S increase, the velocity profile graph decreases. Similarly, the velocity graph decreases as the values of velocity slip parameter A increase. Figs. 3(a-c) presents the variation of temperature profile for different values of magnetic field parameter (M), mass suction parameter (S) ad velocity slip parameter (A). Fig. 3(a) shows the influence of M on the thermal field. Transverse magnetic field has increased the thermal boundary layer thickness. However, an increment in thermal boundary layer is not significant amount. Similar to other common fluids, the nanofluid shows similar characteristics regarding the influences of magnetic field on thermal field. Fig. 3(b) displays the variation of temperature with S. As the values of S increase, the temperature graph is decreasing. Moreover, the thermal boundary layer thickness ad surface temperature is also decreasing. Fig. 3(c) displays the variation of temperature with A. As the values of A increase, the temperature graph is increasing. Since the temperature equation is coupled with velocity function, the increasing values of velocity slip parameter enhances the thermal boundary layer thickness ad surface temperature is also increasing. Figs. 4(a-c) presents the variation of temperature profile for different values of thermal slip parameter (B), radiation parameter (R) ad Prandtl number (P_r). Fig. 4(a) shows the variation of temperature with respect to B. The graph reveals that the wall temperature $\theta'(0)$ ad thermal boundary layer thickness decreases when the values of B increases. However, the opposite effect is true with the radiation parameter R as shown in Fig. 4(b). As the values of R increase, the thermal boundary layer thickness increases. This may be due to the reduction of rate of heat transfer at the surface. The effect of Prandtl number (P_r) on the heat transfer process is shown by the Fig. 4(c). This figure reveals that an increase in Prandtl number (P_r) results in a decrease in the temperature distribution, because, thermal boundary layer thickness decreases with an increase in (P_r). In short, an increase in the Prandtl number means slow rate of thermal diffusion. The graph also shows that as the values of (P_r) increase, the wall temperature decreases. The effect of (P_r) on a nanofluid is similar to what has already been observed in common fluids qualitatively but they are different quantitatively. Therefore, these properties are inherited by nanofluids. Figs. 5(a-c) presents the variation of temperature profile for different values of Eckert number (E_c), thermophoresis parameter (N_t) ad Brownian motion parameter (N_b). Fig. 5(a) illustrates the influence of (E_c) on temperature in the boundary layer. On observing the temperature graph, the wall temperature of the sheet increases as the values of (E_c) increase. Moreover, when the

values of (E_c) increase, the thermal boundary layer thickness increases near the boundary ad then decreases asymptotically. Fig. 5(b, c) shows the influence of the change of (N_b) ad (N_t) on temperature profile when $(N_b = N_t = 0)$. It is noticed that as thermophoresis parameter increases the thermal boundary layer thickness increases and the temperature gradient at the surface decrease (in absolute value) as both (N_b) ad (N_t) increase. Therefore, the local Nusselt number $-\theta'(0)$, which represents the heat transfer rate at the surface, decreases. Consequently, temperature on the surface of a sheet increases. This is due to the fact that the thermophoresis Parameter (N_t) is directly proportional to the heat transfer coefficient associated with the fluid. Figs. 6(a-c) presents the variation of concentration profile for different values of magnetic field parameter (M), mass suction parameter (S) ad solutal slip parameter (c).For increasing values of (M),the concentration profile gets decelerated which ca be observed in case (a). On the other had the suction parameter (S) has a strong influence on the concentration profile as it is shown in case (b). As the values of suction parameter (S) increase, concentration graph decreases ad the concentration boundary layer thickness decreases. Fig. 6 (c) illustrates the variation of concentration with respect to concentration slip parameter (c). As it ca be seen from the graph, the concentration slip parameter does not have any influences on concentration profile graph. Figs. 7(a-c) presents the variation of concentration profile for different values of Lewis number (L_e), radiation parameters (R) ad Prandtl number (P_r). It is noticed from Fig. 7(a) that as Lewis number increases the concentration graph decreases ad the concentration boundary layer thickness decreases. This is probably due to the fact that mass transfer rate increases as Lewis number increases. It also reveals that the concentration gradient at surface of the sheet increases. Moreover, the concentration at the surface of a sheet decreases as the values of (L_e) increase. Fig. 7(b) illustrates the variation of radiation parameters (R) on concentration graph. The influences of radiation parameter on concentration is not this much significant. As the values of radiation parameter R increase, the concentration boundary layer thickness is not changing much. Fig. 7 (c) reveals the variation of Prandtl number (P_r) on concentration profile. It is noticed that as (P_r) increases, solutal boundary layer increases near the boundary but then after, it gets decelerated. Figs. 8(a-c) presents the variation of concentration profile for different values of Eckert number (E_c), thermophoresis parameter (N_t) and Brownian motion parameter (N_b). Fig. 8 (a) is the evidence of increased solutal boundary layer for increased values of (E_c). Fig. 8(b) reveals the variation of concentration graph in response to a change in thermophoresis parameter (N_t). The influence of thermophoresis parameter on concentration profile graph is monotonic, i.e. as the values of (N_t) increase, the concentration boundary layer thickness is also increasing. Fig. 8(c) reveals the variation of concentration in response to a change in Brownian motion parameter (N_b). As the values of Brownian motion parameter increase, the concentration boundary layer thickness is decreasing. The variation of local skin friction coefficient is displayed in Fig. 9(a-c) for increasing values of magnetic field parameter (M), mass suction parameter (S) ad velocity slip parameter (A).For increasing (M), skin friction coefficient increases but reverse trend is observed for both (S) ad (A) .The variation of local Nusselt number is displayed in Figs. 10-12 for increasing values of governing parameters i.e., magnetic field parameter (M), mass suction parameter (S), velocity slip parameter (A), thermal slip parameter (B), radiation parameters (R), Prandtl number (P_r), Eckert number (E_c), thermophoresis parameter (N_t) ad Brownian motion parameter (N_b). It is noticed, for the cases of M, A, P_r, E_c, N_t and N_b,Nusselt number is increased but a reverse trend is occurred for B, S and R. The variation of local Nusselt number is displayed in Figs. 10-12 for increasing values of governing parameters i.e., magnetic field parameter (M), mass suction parameter (S), solutal slip parameter (c), radiation parameters (R), Prandtl number (P_r),Lewis number (L_e),Eckert number (E_c), thermophoresis parameter (N_t) ad Brownian motion parameter (N_b). It is noticed, for the cases of M, S, c, P_r, E_c and N_t,Nusselt number is increased but a reverse trend is occurred for L_e, R and N_b.

CONCLUSION

The main findings of the study are summarized as follows:

Velocity profiles decrease with an increase in M. The thickness of velocity boundary layer decreases with an increase in magnetic field parameter M. The velocity at the surface of a sheet decreases as the values of A increase. Thermal boundary layer thickness decreases with an increase in values of slip parameter B ad Prandtl number P_r. The thickness of thermal boundary layer increases with an increase in radiation parameter R, magnetic field parameter M ad thermophoresis parameter N_t when $N_t = N_b$. An increase in parameter N_b decreases the local Nusslet number but the opposite is true in local Sherwood number. The wall temperature gradient increases with an increase in Lewis Number L_e and Prandtl number P_r. The surface temperature of a sheet increases with radiation parameter R but it decreases with an increase in Prandtl number P_r. Concentration boundary layer thickness decreases with an increase in Lewis number L_e ad N_b but increases with an increase in N_t. The skin friction coefficient increases as the values of velocity slip parameter A increases.

Fig.2 Variation of Velocity Profile f ' (η)

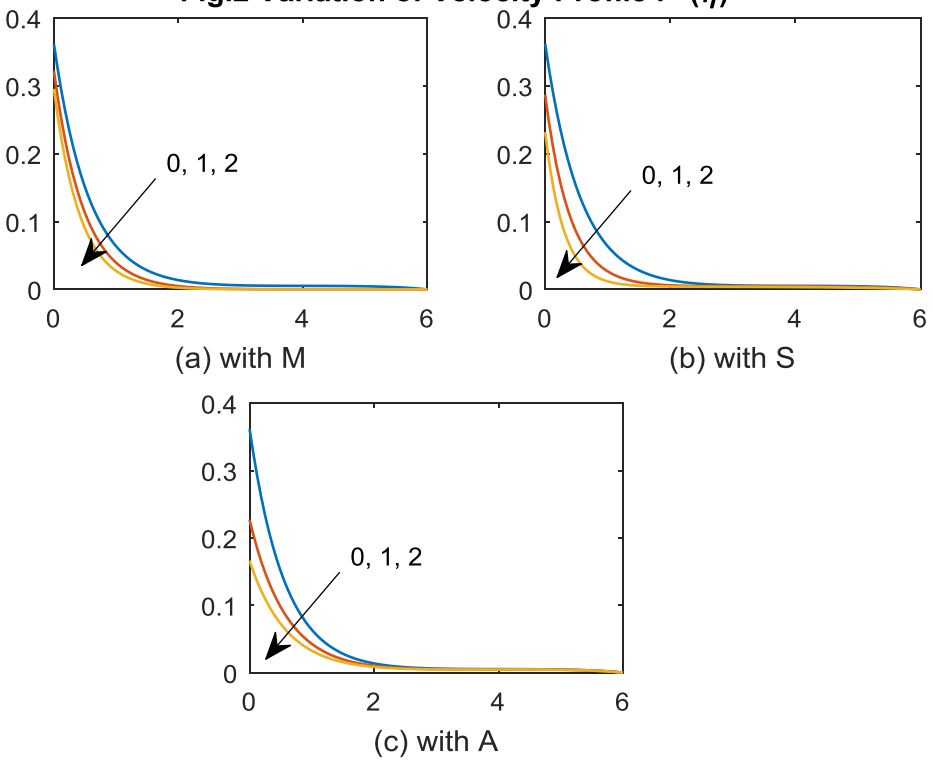

Fig.3 Variation of Temperture Profile $\theta(\eta)$

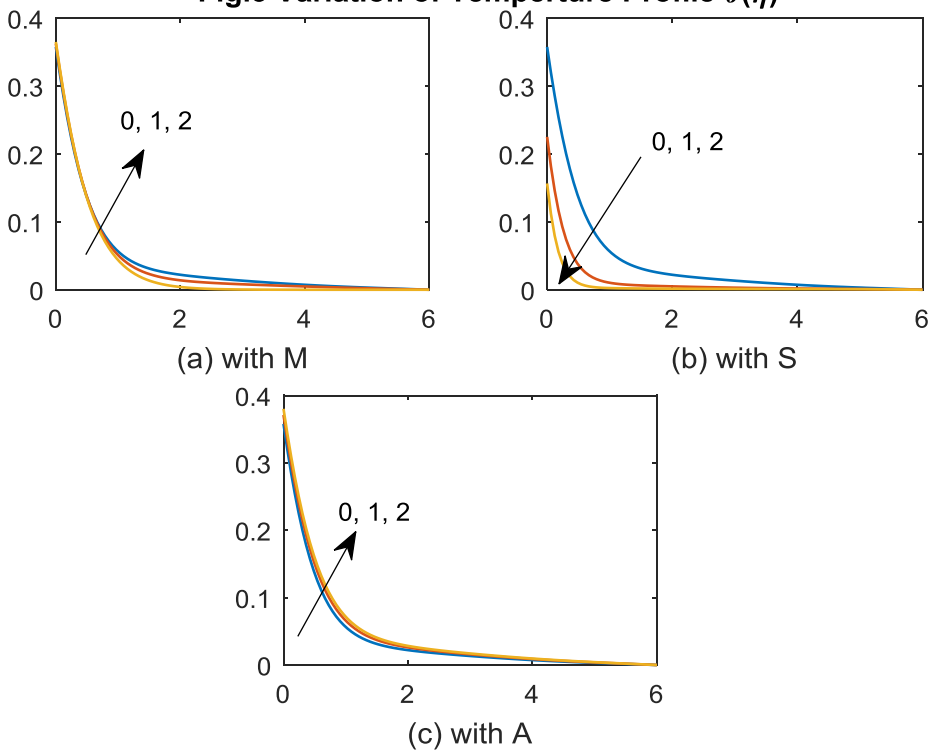

Fig.4 Variation of Temperture Profile $\theta(\eta)$

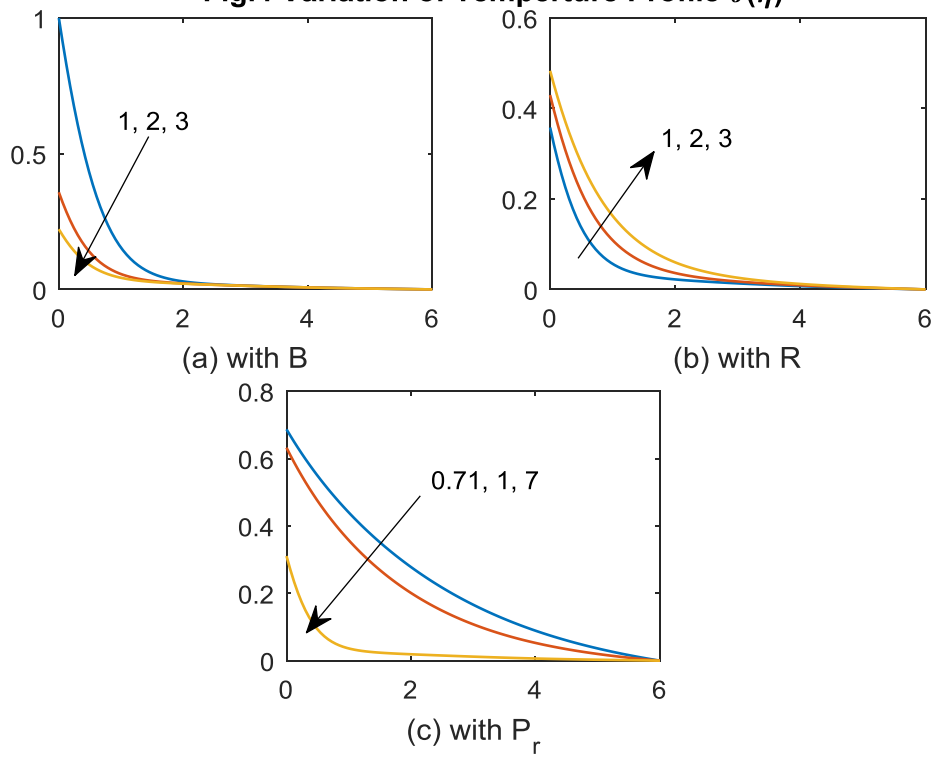

Fig.5 Variation of Temperture Profile $\theta(\eta)$

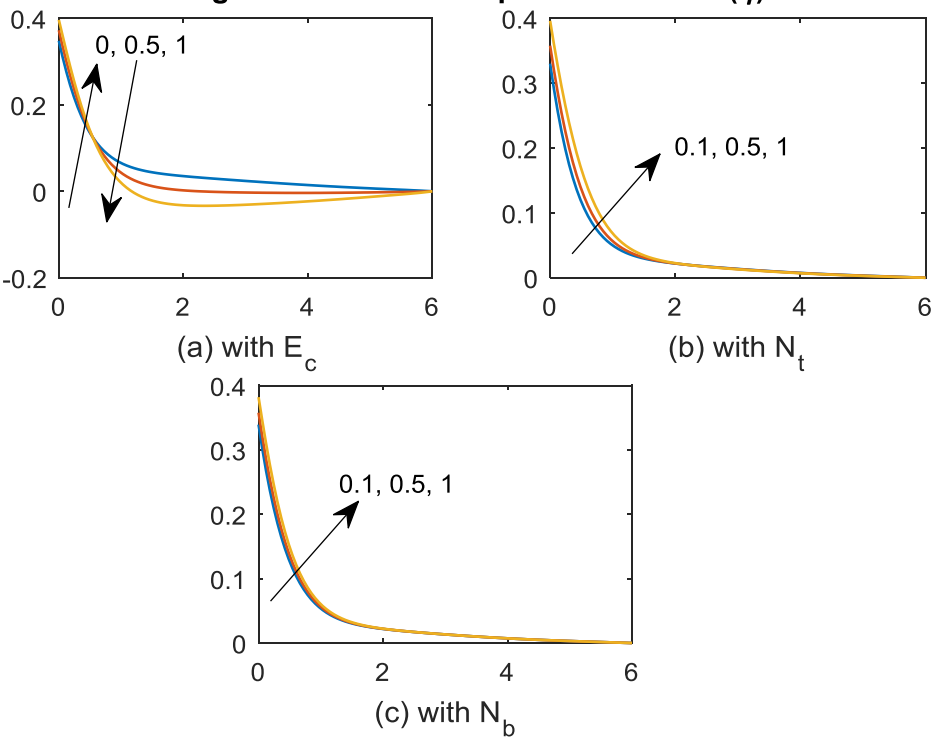

Fig.6 Variation of Concentration Profile $\phi(\eta)$

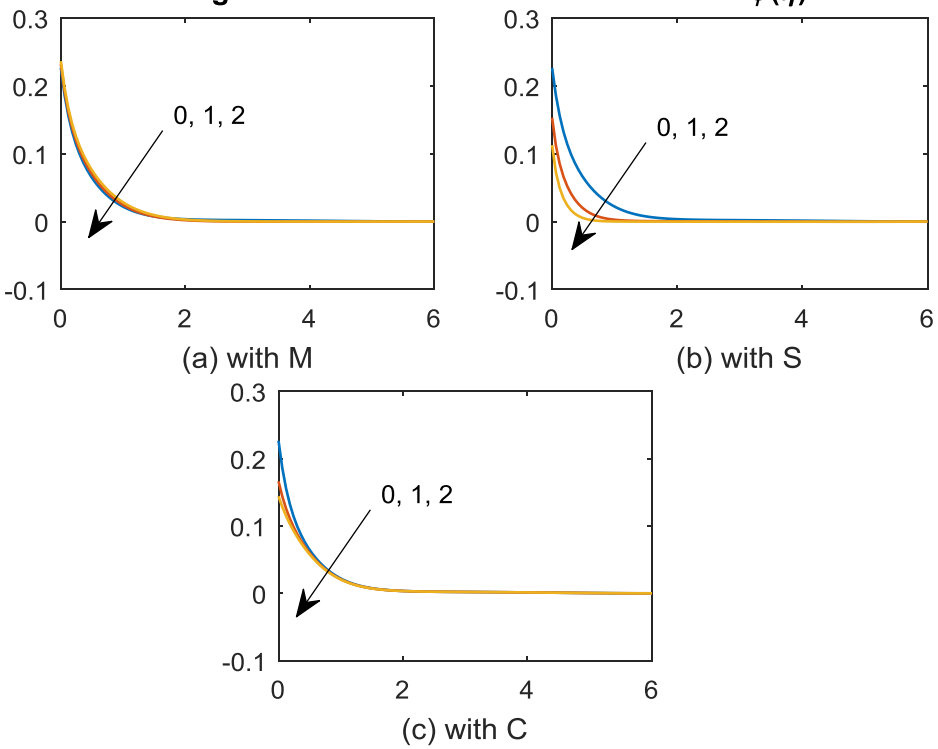

Fig.7 Variation of Concentration Profile $\phi(\eta)$

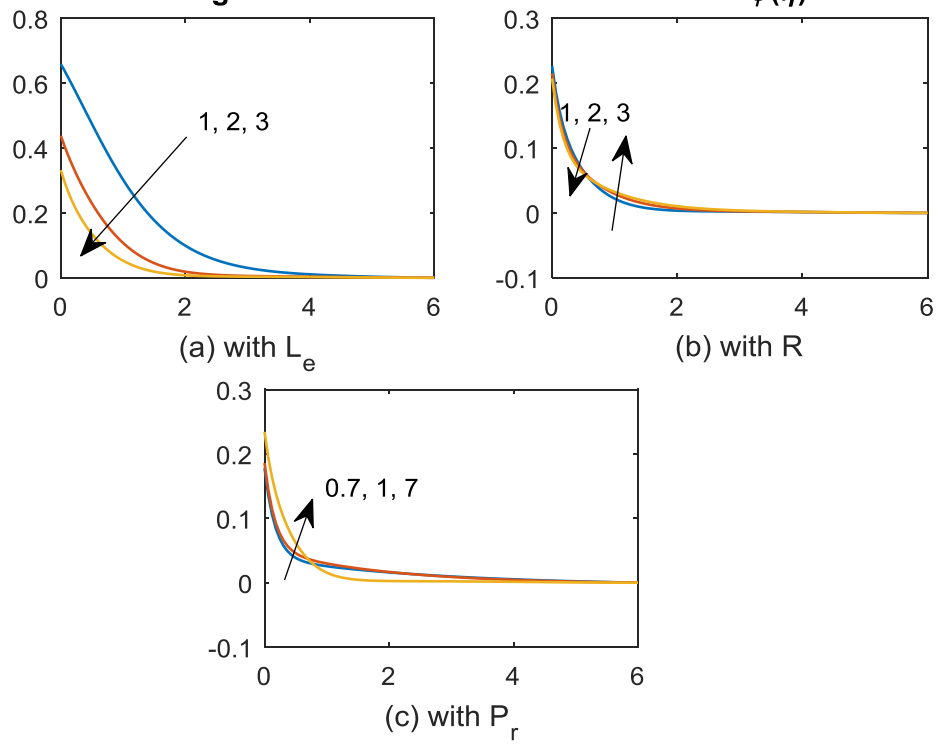

Fig.8 Variation of Concentration Profile $\phi(\eta)$

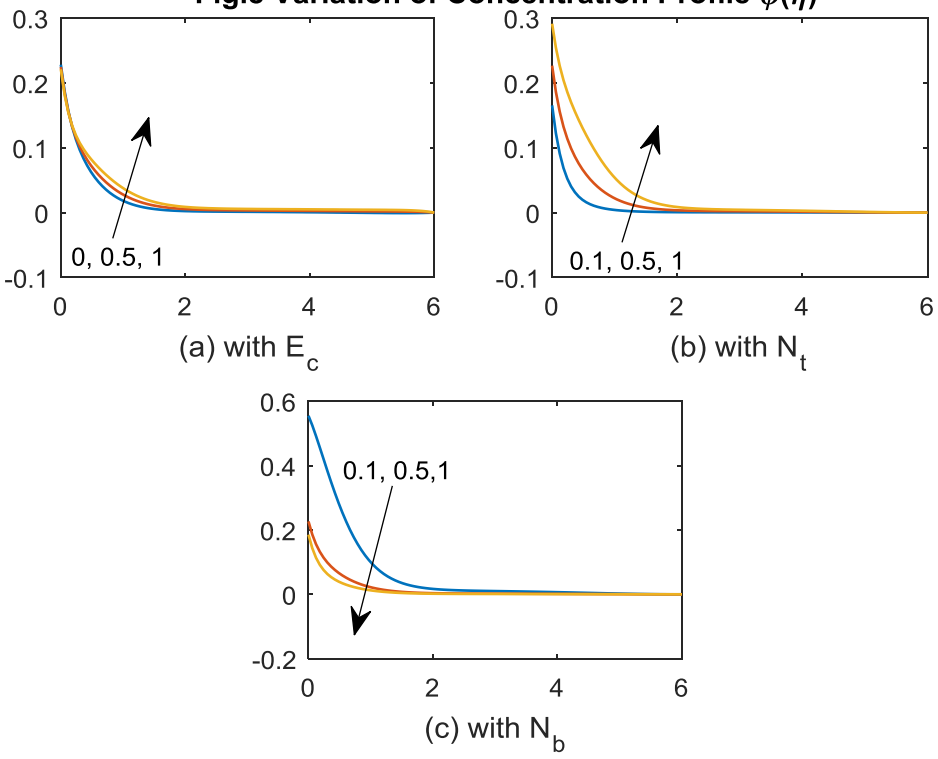

Fig.9 Variation of Skin friction coefficient C_f

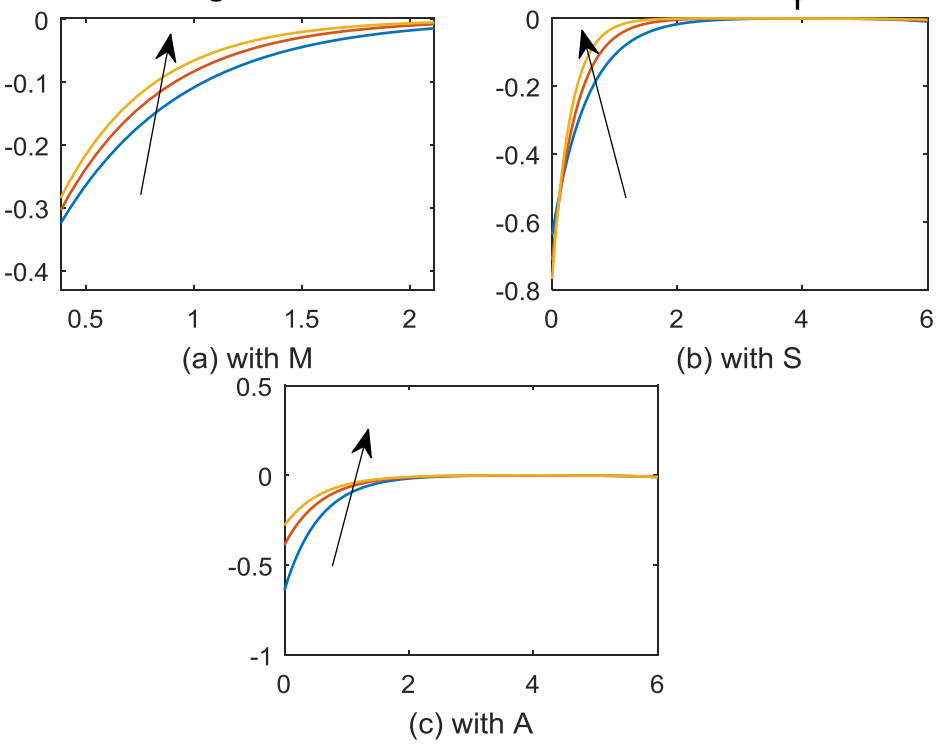

Fig.10 Variation of Nusselt Number Nu_x

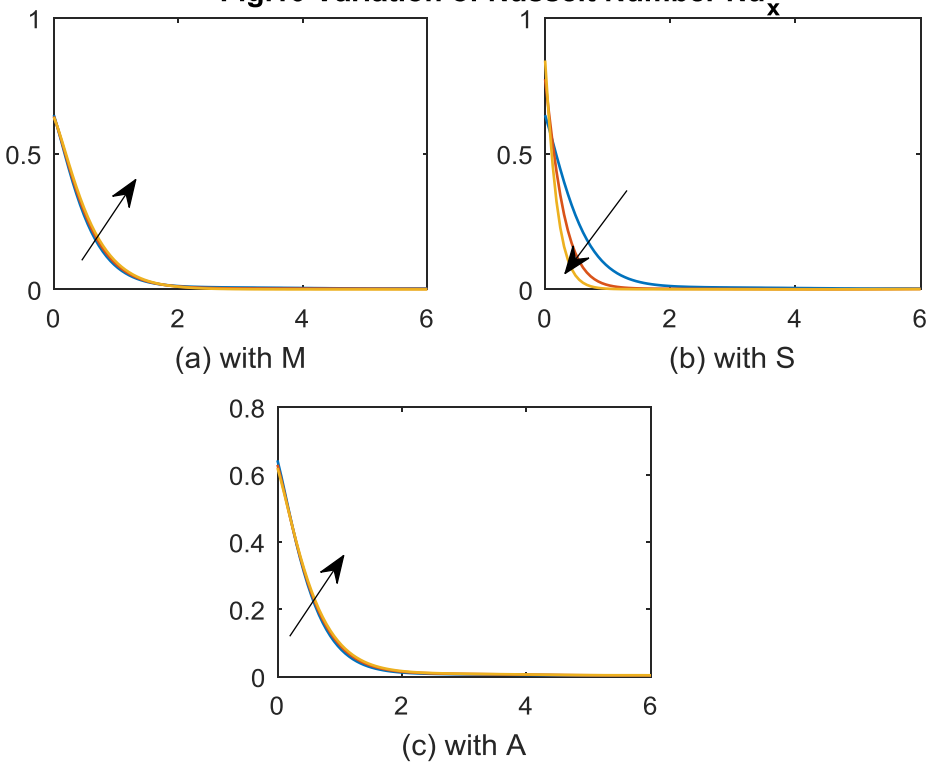

Fig.11 Variation of Nusselt Number Nu_x

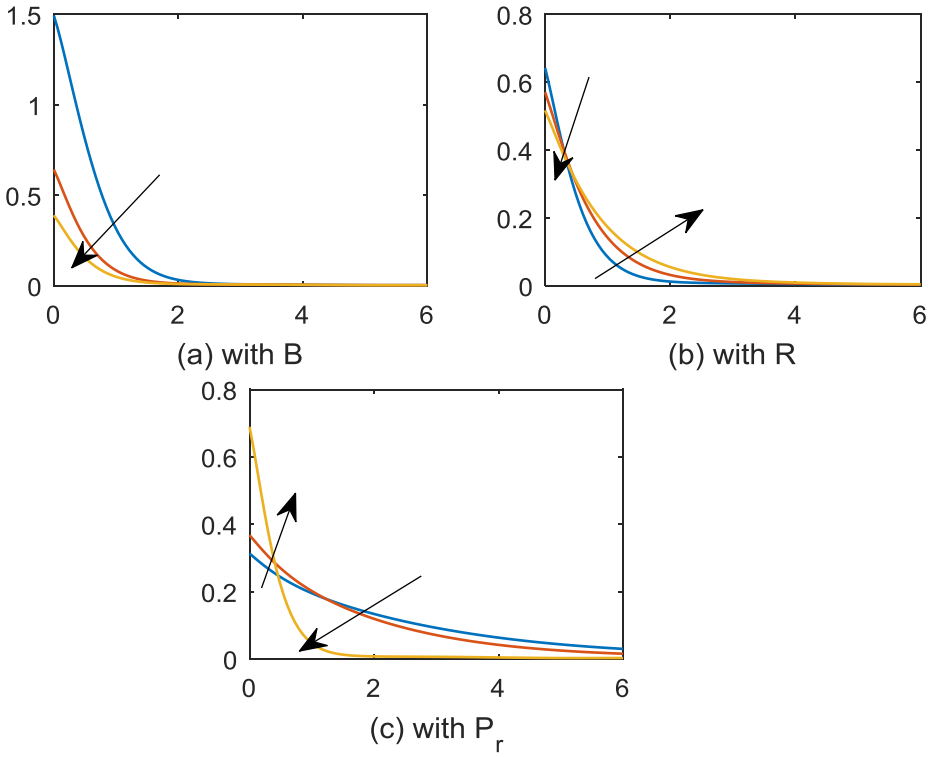

Fig.12 Variation of Nusselt Number Nu_x

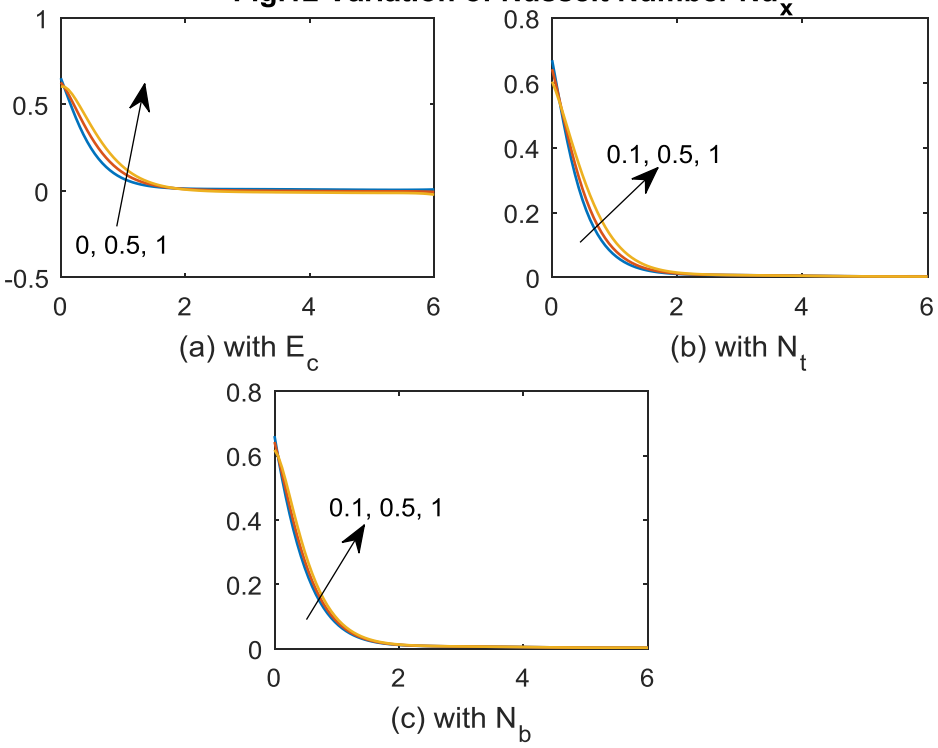

(a) with E_c (b) with N_t

(c) with N_b

Fig.13 Variation of Sherwood Number Sh_x

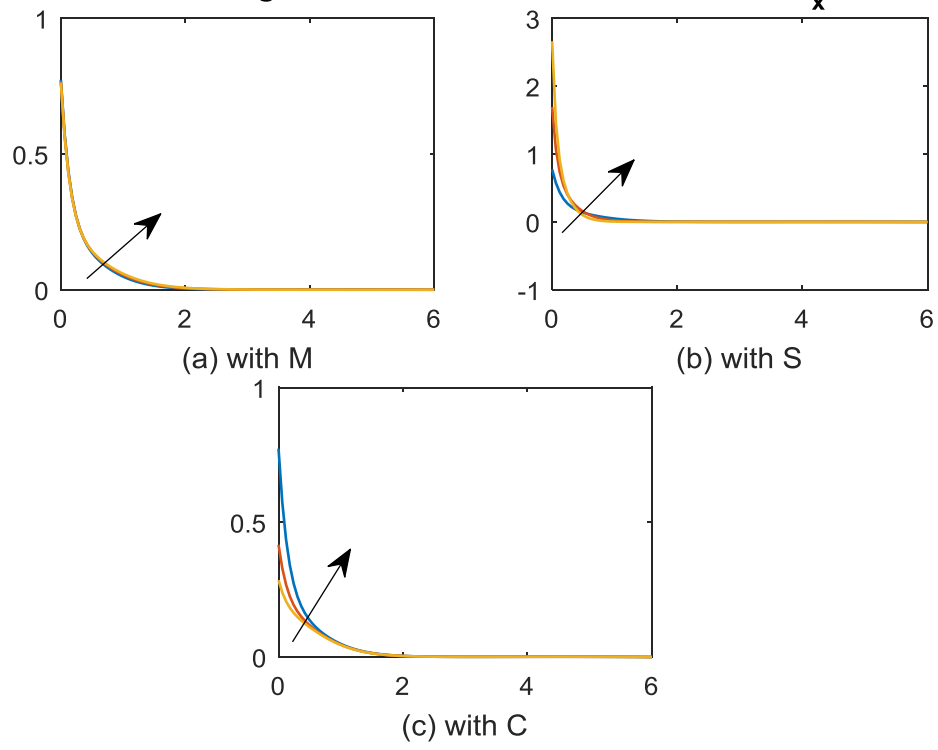

(a) with M (b) with S

(c) with C

Fig.14 Variation of Sherwood Number Sh_x

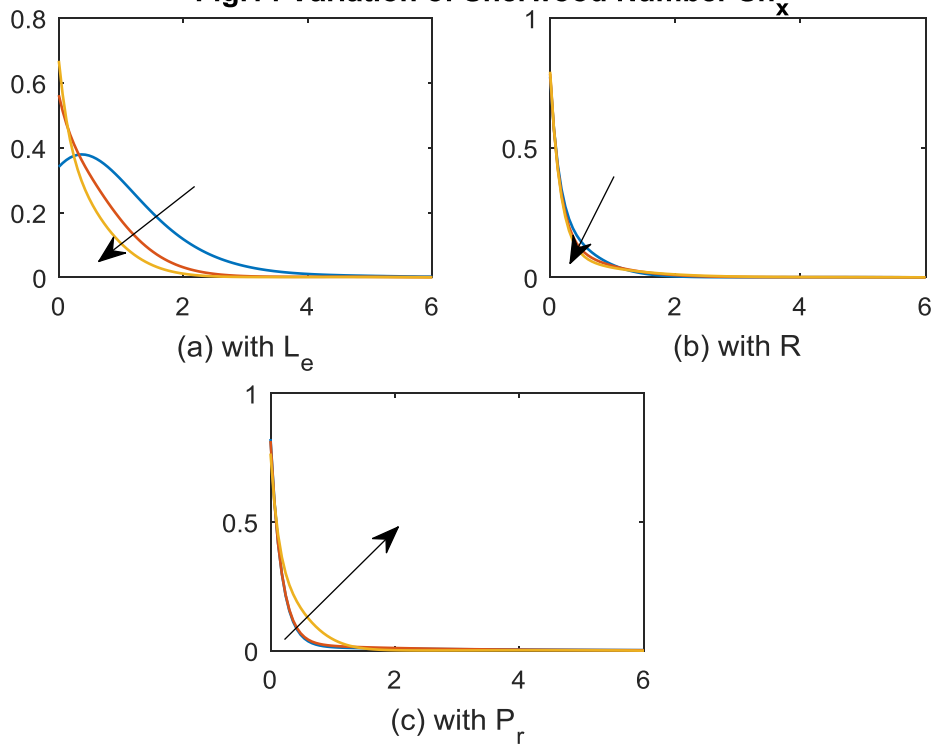

Fig.15 Variation of Sherwood Number Sh_x

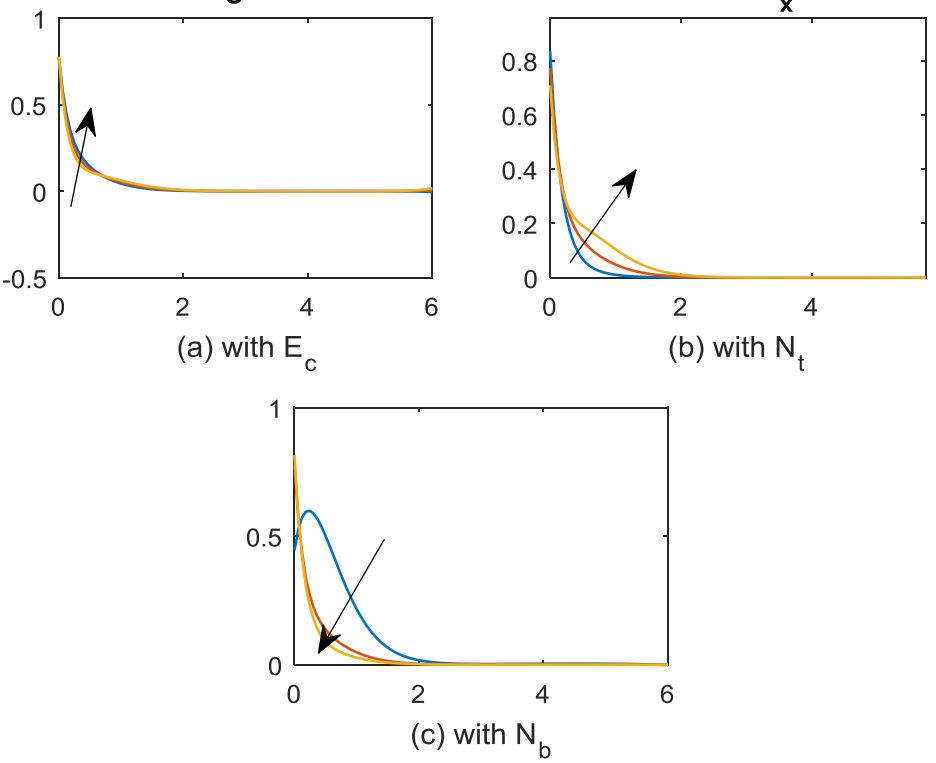

REFERENCES

1. *Sakiadis BC. Boundary layer behavior on continuous solid surface: II. The boundary layer on a continuous flat surface. J Am Ins Chem Eng 1961;7(2):221–5.*
2. *Aderson H. Slip flow past a stretching surface. Acta Mech 2002;158:121–5.*
3. *Wag CY. Flow due to a stretching boundary with partial slip-an exact solution of the Navier–Stokes equation. Chem Eng Sci 2002;57:3745–7.*
4. *Wag CY. Stagnation slip flow ad heat transfer on a moving plate. Chem Eng Sci 2006;61:7668–72.*
5. *Fag T, Zhag J, Yao S. Slip MHD viscous flow over a stretching sheet – an exact solution. Commun Non-linear Sci Numer Simul 2009;14:3731–7.*
6. *Hayat T, Qasim M, Mesloub S. MHD flow ad heat transfer over permeable stretching sheet with slip conditions. Int J Numer Meth Fluid 2011;66:963–75.*
7. *Aziz A. Hydrodynamic ad thermal slip flow boundary layer over a flat plate with constant heat flux boundary condition. Commun Non-linear Sci Numer Simul 2010;15:573–80.*
8. *Fag T, Yao S, Zhag J, Aziz A. Viscous flow over a shrinking sheet with second order slip flow model. Commun Non-linear Sci Numer Simul 2010;15:1831–42.*
9. *Mahatesh M, Vajravelu K, Abel MS, Siddalingappa MN. Second order slip flow ad heat transfer over a stretching sheet with non-linear Navier boundary condition. Int J Therm Sci 2012;58:142–50.*
10. *Keblinski P, Eastma JA, Cahaill DG. Nanofluids for thermal trasport. Mater Today 2005;8(6):36–44.*
11. *Choi S. Enhacing thermal conductivity of fluids with nanoparticle. In: Development and applications of non-Newtonian flow. ASME, FED-vol.231/ MD-vol.66; 1995. p. 99–105.*
12. *Eastma JA, Choi SUS, Li S, Yu W, Thompson LJ. Aomalously increased effective thermal conductivity of ethylene glycol-based nanofluids containing copper nanoparticles. Appl Phys Lett 2001;78(6):718–20.*
13. *Choi SUS, Zhag ZG, Yu W, Lockwoow FE, Grulke EA. Aomalous thermal conductivities enhacement on nanotube suspension. Appl Phys Lett 2001;79:2252–4.*
14. *Kuznetsov AV, Nield DA. Natural convective boundary-layer flow of a nanofluid past a vertical plate. Int J Therm Sci 2010;49:243–7.*
15. *Kha WA, Pop I. Boundary layer flow of a nanofluid past a stretching sheet. Int J Heat Mass Transfer 2010;53:2477–83.*
16. *Ibrahim W, Shaker B. Boundary-layer flow ad heat transfer of nanofluid over a vertical plate with convective surface boundary condition. J Fluid Eng-Tras ASME 2012:134. 081203-1.*
17. *Haddad Z, Nada A, Oztop F, Mataoui A. Natural convection in nanofluids: are the thermophoresis ad Brownian motion effect significant in nanofluids heat transfer enhancement? Int J Therm Sci 2012;57:152–62.*
18. *Bachok N, Ishak A, Pop I. Boundary-layer flow of nanofluids over a moving surface in a flowing fluid. Int J Therm Sci 2010;49:1663–8.*
19. *Makinde OD, Aziz A. Boundary layer flow of a nanofluid past a stretching sheet with convective boundary condition. Int J Therm Sci 2011;50:1326–32.*
20. *Vajravelu K, Prasad KV, Jinho L, Chaghoon L, Pop I, Robert A, et al. Convective heat transfer in the flow of viscous Ag–water ad Cu–water nanofluids over a stretching surface. Int J Therm Sci 2011;50:843–51.*
21. *Hamad A, Ferdows M. Similarity solution of boundary layer stagnation point flow towards a heated porous stretching sheet saturated with nanofluid with heat absorption/generation ad suction/blowing: a lie group analysis. Commun Non-linear Sci Numer Simul 2012;17:132–40.*
22. *Mostafa M, Hayat T, Pop I, Asghar S, Obaidat S. Stagnation point flow of a nanofluid towards a stretching sheet. Int J Heat Mass Transfer 2011;54:5588–94.*
23. *Ibrahim W, Shaker B, Mahantesh M. MHD stagnation point flow ad heat transfer due to nanofluid towards a stretching sheet. Int J Heat Mass Transfer 2013;56:1–9.*
24. *Hamad MA, Pop I, Ismali AI. Magnetic field effects on free convection flow of a nanofluid past a vertical semi-infinite flat plate. Non-Linear Aal: Real World Appl 2011;12:1338–46.*
25. *Yacob A, Ishak A, Pop I, Vajravelu K. Boundary layer flow past a stretching/shrinking surface beneath an external uniform shear flow with convective surface boundary condition in a nanofluid. Nanoscale Res Lett2011;6(314):1–7.*
26. *Turkyilmazoglu M. Exact aalytical solution for heat and mass transfer of MHD slip flow in nanofluids. Chem Eng Sci 2012;84:182–7.*
27. *Uddin MJ, Kha WA, Ismail AIMd. Scaling group transformation for MHD boundary layer slip flow of a nanofluid over a convectively heated stretching sheet with heat generation mathematical problems in engineering, vol. 2012. article ID 934964.*
28. *Wag X, Mujumdar AS. A review on nanofluids – Part I: Theoretical ad numerical investigation. Braz J Chem Eng 2008;25(04):613–30.*
29. *Wag X, Mujumdar AS. A review on nanofluids-part ii: experiments ad applications. Braz J Chem Eng 2008;25(04):631–48.*
30. *Aminreza N, Pourajab R, Ghalambaz M. Effect of partial slip boundary condition on the flow ad heat transfer of nanofluids past stretching sheet prescribed constant wall temperature. Int J Therm Sci 2012;54:253–61.*
31. *Kalidas D. Slip flow ad convective heat transfer of nanofluids over a permeable stretching surface. Comput Fluids 2012;64:34–42.*
32. *Pattnaik P K ad Biswal T,MHD free convective boundary layer flow of a viscous fluid at a vertical surface through porous media with non-uniform heat source, IJISET,2(3)(2015).*
33. *Pattnaik P K, Biswal T, Analytical solution of mhd free convective flow through porous media with time dependent temperature ad concentration, Walailak J Sci & Tech, 12 (9) (2015) 749-762.*
34. *Pattnaik P K, Mishra S R, Bhatti M M, Abbas T, Analysis of heat and mass transfer with MHD and chemical reaction effects on viscoelastic fluid over a stretching sheet, India J Phys(2017), DOI 10.1007/s12648-017-1022-2.*
35. *Pattnaik P K, Mishra S R, Dash G C, Effect of heat source and double stratification on MHD free convection in a micropolar fluid, Alexadria Engineering Journal, 54 (2015) 681–689.*
36. *P. K. Pattnaik, N. Mishra, M. M. Muduly, N. B. Mohapatra, Effect of chemical reaction on nanofluid flow over a unsteady stretching sheet in presence of heat source, Pramaa Research Journal, 8 (8) (2018)142-166.*